Available online at www.sciencedirect.com
ScienceDirect
Journal of Molecular Graphics and Modelling 26 (2008) 1252–1258
Journal of Molecular Graphics and Modelling
www.elsevier.com/locate/JMGM

Three-dimensional holographic vector of atomic interaction field for quantitative structure–activity relationship of Aza-bioisosteres of anthrapyrazoles (Aza-APs)

Xu Luo-nan [a,b,*], Liang Gui-Zhao [b], Li Zhi-liang [a,b,*], Wang Juan [a], Zhou Peng [a]

[a] College of Chemistry and Chemical Engineering, Chongqing University, Chongqing 400044, China
[b] College of Bioengineering, Key Laboratory of Biomedical Engineering of Educational Ministry and Chongqing City, Chongqing 400044, China

Received 1 July 2007; received in revised form 20 November 2007; accepted 24 November 2007
Available online 4 December 2007

Abstract

A newly developed descriptor, three-dimensional holographic vector of atomic interaction field (3D-HoVAIF), is used to describe the chemical structures of Aza-bioisosteres of anthrapyrazoles (Aza-APs). 3D-HoVAIF contains three non-bonded (electrostatic, van der Waals and hydrophobic) factors, which are directly related to bioactivities and utilized to express intramolecular potential energies, employed to several different models on 35 anticancer agents Aza-APs. After variable screening by stepwise multiple regression (SMR) technique, a partial least square (PLS) regression model is built with 3D-HoVAIF. The model is satisfactory comparing to reference since correlation coefficients of molecular modeling (R^2), cross-validation (q^2) and standard deviation of estimation (S.D.) are 0.865, 0.722 and 0.299, respectively, showing that the model has favorable estimation and prediction capabilities. It is illustrated that information related to the anticancer activity of Aza-APs could preferably be expressed by 3D-HoVAIF with definite physicochemical meanings and easy structural interpretation for Aza-APs. 3D-HoVAIF is proved to be potent in relation with bioactivities, while overcoming many demerits of traditional 3D structural characterization methods.

Keywords: Three-dimensional holographic vector of atomic interaction field (3D-HoVAIF); Quantitative structure–activity relationship (QSAR); Aza-bioisosteres of anthrapyrazoles (Aza-APs)

1. Introduction

Recently studies show that Aza-bioisosteres of anthrapyrazoles (Aza-APs) show anticancer activity, which correlates with the ability of the agents to influence the speed of DNA cleavage mediated by the enzyme topoisomerase II [1–5]. This family of compounds is structurally related to mitoxantrone (MX), whose mechanism of action is mainly related to the poisoning of the DNA topoisomerase II enzyme [6,7], but the major problem with the clinical use of MX and congeners is related to cardiotoxic effects [8]. In a previous investigation, combining the approaches of bioisosteric substitution with pyrazole introduction into the anthraquinone system led to the design of Aza-anthrapyrazoles. C–N substitutions were introduced at different positions of the anthrapyrazole ring system, giving different regioisomers [9]. Interestingly, and in analogy to Aza-anthracenediones, the cytotoxic properties of these derivatives were substantially affected by the location of the bioisosteric nitrogen. In fact, only 9-Aza derivatives showed outstanding activity both in vitro and in vivo. In vitro evaluation of 9-Aza-APs demonstrated high cytotoxic potency against the human colon tumor cell line LoVo and the ability of overcoming multidrug resistance induced in a doxorubicin-resistant cell line [10]. The compounds showed also outstanding in vivo antitumor activity against both systemic P388 murine leukemia and MX-1 human mammary carcinoma transplanted in nude mice. These agents are structurally similar to the anthracenedione MX and LX. Their mechanism of action was studied by Sissi et al. [11]. The authors showed that the 9-Aza-APs exhibit prominent affinity for DNA and established an important electrostatic contribution to the binding free energy.

* Corresponding authors.
E-mail addresses: xln911s@yahoo.com.cn (X. Luo-nan), zlli-cqu@163.com (L. Zhi-liang).

1093-3263/$ – see front matter © 2007 Elsevier Inc. All rights reserved.
doi:10.1016/j.jmgm.2007.11.007

The compounds possess a strong preference for GC base pairs in the double-helical DNA. Their common geometry of complex with DNA is distinguished very much from that of MX. Sissi et al. discussed that Aza-bioisosteric derivatives of MX and LX do not stimulate topoisomerase II-mediated DNA cleavage. This was considered as an indication for alternative, non-enzyme mediated mechanism(s) for cell killing, possibly related with redox cycling.

On the basis of their efficacy profile in additional experimental tumors and lack of cardiotoxicity in preclinical models [11], two derivatives from the 9-Aza-APs family, BBR 3438 (2-[2-(2-hydroxy-ethylamino)-ethyl]-5-(2-methylamino-ethylamino)indazolo [4,3-g,h]isoquinoline-6(2H)-one) and BBR 3576 (5-(2-dimethylamino-ethylamino)-2-[2-(2-hydroxy-ethylamino)-ethyl]-indazolo[4,3-g,h] isoquinoline-6(2H)-one), have surfaced as potential clinical candidates, and showed that bioisosteric substitution plays an important role in defining the physicochemical properties and in modulating the affinity of anthrapyrazoles for DNA, the geometry of the intercalation complex and the sequence specific contacts along the DNA chain [12]. In addition, it emerged that drug stimulation of topoisomerase II-mediated DNA cleavage was attenuated in the Aza derivatives when compared to their carbocyclic analogues. The preclinical profile of efficacy against prostatic carcinoma, a tumor resistant to conventional antitumor drugs, makes the novel 9-Aza-APs BBR 3438 a promising candidate for clinical evaluation [13].

In this paper, three-dimensional holographic vector of atomic interaction field (3D-HoVAIF) of 35 9-Aza-APs synthesized and biologically tested by Krapcho et al. [10], to gain more anticancer activity information of this series compounds.

2. Methods and materials

It has been nearly 40 years since the quantitative structure–activity relationship (QSAR) paradigm first found its way into the practice of pharmaceutical chemistry, toxicology, and eventually most facets of chemistry [14]. Nowadays QSAR mainly include two kinds: one is based on molecular two-dimensional (2D) structures and the other on three-dimensional (3D) configurations. For 2D descriptors, since its first appearance in 1947 by Winer [15], a great deal of such other ones, topological structure-bases as Hosoya index [16], Randic index [17] and Balaban index [18] etc., have been consequently developed with remarkable achievements in physicochemical property predictions for organic homologues [19]. Nevertheless, 2D descriptors, impossible to take reflection of molecular actual spatial structures and regardless of ligand-receptor interaction mechanisms, are incapable of constructing effective QSAR models for drug and biological macromolecules. In 1988 following the appearance of CoMFA [20] developed by Cramer, a series of similar methods, based upon molecular spatial potential energy distribution as CoMSIA [21], HASL [22] and GRID analysis [23] etc., have their consequent appearance been the mainstream of modern drug design. Combinating advantages of both 3D methods in explicit, accurate and explainable representation and 2D methods in easy and quick characterization, 3D holographic vector of atomic interaction field, 3D-HoVAIF, proposed by our laboratory, achieved satisfied results in building the QSAR model for Aza-bioisosteres of anthrapyrazoles (Aza-APs).

2.1. Introduction of three-dimensional holographic vector of atomic interaction field (3D-HoVAIF)

2.1.1. Atomic types and interactions

Based on molecular electric-distance vector [17–19], 3D-HoVAIF was developed considering three common non-bonding interactions biological activities, i.e., electrostatic interaction, steric interaction, hydrophobic interaction related with atomic relative distance and atomic self-properties. These descriptors neither resort to any experimental parameters nor consider configuration overlap of samples. Ordinary atoms of organic molecules including H, C, N, P, O, S, Cl, Br, I, which are partitioned into 5 types in the Periodic Table. According to hybridization state of atoms, the atoms are furthermore subdivided into 10 types. Thus, there are 55 interatomic interactions in a molecule (Table 1). In this paper, three kinds of potential energy field, electrostatic, steric and hydrophobic, take part in the representation of different interactions, producing $3 \times 55 = 165$ interaction items for organic molecule.

2.1.2. Atom interaction potential energies

Electrostatic interaction: an important non-bonded interaction obeying Coulomb's law. In Eq. (1), r_{ij} denotes interatomic

Table 1
10 Types of atoms and the resulting 55 types of atomic in 3D-HoVAIF

NO	Atomic Types	1	2	3	4	5	6	7	8	9	10
01	H	1–1	1–2	1–3	1–4	1–5	1–6	1–7	1–8	1–9	1–10
02	C(sp^3)		2–2	2–3	2–4	2–5	2–6	2–7	2–8	2–9	2–10
03	C(sp^2)			3–3	3–4	3–5	3–6	3–7	3–8	3–9	3–10
04	C(sp)				4–4	4–5	4–6	4–7	4–8	4–9	4–10
05	N(sp^3)					5–5	5–6	5–7	5–8	5–9	5–10
06	N(sp^2)						6–6	6–7	6–8	6–9	6–10
07	N(sp)							7–7	7–8	7–9	7–10
08	O(sp^3), S(sp^3)								8–8	8–9	8–10
09	O(sp^2), S(sp^2)									9–9	9–10
10	F, Cl, Br, I										10–10

Euclid distance, with the unit of m; e is the elementary charge ($1.602 \times 189 \times 2 \times 10^{-19}$ C); ε_0 represents dielectric constant $8.854 \times 187 \times 82 \times 10^{-12}$ $C^2/(J\,m)$ in vacuum; Z is the amounts of net electric charges; m and n are atomic type. Electrostatic interactions among all the atoms included in a molecule could be given out by this equation, then accumulating them together into each of the 55 interaction items according to their atom-pair attributes.

$$E_{\mathrm{mn}}(E) = \sum_{i \in m, j \in n} \frac{e^2}{4\pi\varepsilon 0} \frac{Z_i Z_j}{r_{ij}} \quad (1 \le m \le 10, m \le n \le 10) \tag{1}$$

Steric interaction is described by Lennard-Jones formula (Eq. (2)). Amongst, $\varepsilon_{ij} = (\varepsilon_{ii}\varepsilon_{jj})^{1/2}$ is potential well of atomic pairs, with its value taken from Ref. [21]; $R_{ij}^3 = (-ChR_{ii}^3 + ChR_{jj}^3)/2$, is van der Waals' radius for modified atom-pair, with corrected factor Ch of 1.00 in case of sp^3 hybridization, 0.95 sp^2 hybridization and 0.90 sp hybridization [22].

$$E_{mn}(S) = \sum_{i \in m, j \in n} \varepsilon_{ij} D \left[\left[\frac{R_{ij}}{r_{ij}} \right]^{12} - 2 \left[\frac{R_{ij}}{r_{ij}} \right]^{6} \right] \tag{2}$$
$$(1 \le m \le 10, m \le n \le 10)$$

Hydrophobic interaction force field is defined as interatomic hydrophobic interaction in Hint method proposed by Kellogg et al. [23]. Amongst, S is the solvent accessible surface area (SASA) for atoms [24], indicating information on surface area when water-molecule probe roiling its sphere at the atomic surface; a is atomic hydrophobic constant, taken the value from Ref. [25]; T is sign function, indicating entropy change resulting from different types of atomic interaction [26–30].

$$E_{\mathrm{mn}}(H) = \sum_{i \in m, j \in n} S_i a_i S_j a_j e^{-r_{ij}} T_{ij} \tag{3}$$
$$(1 \le m \le 10, m \le n \le 10)$$

Table 2
Name and IC_{50} activity of thirty-five 9-Aza-APs

No.	R1	R2	$\log(IC_{50})^a$	$\log(IC_{50})^b$	$\log(IC_{50})^c$	$\log(IC_{50})^d$
1	$CH_2CH_2N_2$	$CH_2CH_2NMe_2$	−0.034	−0.224	−0.258	−0.223
2	$CH_2CH_2NMe_2$	$CH_2CH_2NH_2$	−0.340	−0.404	−0.453	−0.242
3	$CH_2CH_2NH_2$	CH_2CH_2NHMe	−1.084	−0.202	0.009	−0.017
4	$CH_2CH_2NMe_2$	$CH_2CH_2NHCH_2CH_2OH$	−0.295	−0.389	−0.451	−0.572
5	$CH_2CH_2NMe_2$	$CH_2CH_2NEt_2$	−0.041	−0.017	−0.133	0.064
6	$CH_2CH_2NMe_2$	2-(4-morpholinyl)ethyl	0.506	0.425	0.595	0.354
7	$CH_2CH_2NMe_2$	$CH_2CH_2CH_2NMe_2$	−0.075	−0.259	−0.709	−0.376
8	$CH_2CH_2NMe_2$	$CH_2CH_2CH_2NH_2$	0.656	0.543	0.474	0.138
9	$CH_2CH_2NMe_2$	2-(1-piperidinyl)ethyl	−0.078	−0.191	−0.359	−0.0776
10	$CH_2CH_2NMe_2$	2-(1-piperidinyl)ethyl	1.061	1.114	1.188	1.061
11	$CH_2CH_2NMe_2$	CH_2CH_2OH	−0.041	−0.010	0.392	0.216
12	$CH_2CH_2NMe_2$	$CH_2CH_2N(CH_2CH_2OH)_2$	0.686	0.605	0.591	0.813
13	$CH_2CH_2NMe_2$	2-(imidazol-1-yl)ethyl	0.438	0.440	−0.376	0.436
14	$CH_2CH_2NMe_2$	$CH_2CH_2N(Me)CH_2CH_2OH$	−0.921	−0.777	−0.927	−0.986
15	$CH_2CH_2NMe_2$	$CH_2CH_2NHSO_2$ Me	0.981	0.938	0.892	0.933
16	$CH_2CH_2NMe_2$	$CH_2CH_2NHCH_2CH_2NMe_2$	0.880	0.874	0.886	0.882
17	$CH_2CH_2NH_2$	$CH_2CH_2NMe_2$	−0.067	−0.239	−0.270	−0.224
18	$CH_2CH_2NH_2$	$CH_2CH_2NH_2$	0.426	−0.037	−0.119	−0.0332
19	$CH_2CH_2NH_2$	CH_2CH_2NHMe	−0.205	−0.441	−0.512	−0.224
20	$CH_2CH_2NH_2$	$CH_2CH_2NHCH_2CH_2OH$	0.648	0.441	0.043	0.146
21	$CH_2CH_2NH_2$	$CH_2CH_2NEt_2$	0.138	0.307	0.369	0.305
22	$CH_2CH_2NH_2$	2-(4-morpholinyl)ethyl	0.652	0.731	0.744	0.528
23	$CH_2CH_2NH_2$	$CH_2CH_2N(CH_2CH_2OH)_2$	2.053	2.084	2.292	2.056
24	$CH_2CH_2NHCH_2CH_2OH$	$CH_2CH_2NMe_2$	−0.119	0.056	0.327	0.529
25	$CH_2CH_2NHCH_2CH_2OH$	$CH_2CH_2NH_2$	0.772	0.577	0.444	0.590
26	$CH_2CH_2NHCH_2CH_2OH$	CH_2CH_2NHMe	0.152	0.155	0.183	0.443
27	$CH_2CH_2NHCH_2CH_2OH$	$CH_2CH_2NHCH_2CH_2OH$	1.040	1.099	1.399	1.088
28	$CH_2CH_2NHCH_2CH_2OH$	$CH_2CH_2N(CH_2CH_2OH)_2$	2.342	2.338	1.522	2.24
29	$CH_2CH_2NHCH_2CH_2OH$	CH_2CH_2OH	2.160	2.157	1.731	1.919
30	$CH_2CH_2CH_2NMe_2$	$CH_2CH_2NMe_2$	−0.214	−0.138	−0.206	−0.572
31	$CH_2CH_2CH_2NMe_2$	$CH_2CH_2NHCH_2CH_2OH$	−0.134	0.081	0.379	−0.0532
32	CH_2CH_2NHMe	CH_2CH_2NHMe	−0.942	−0.576	−0.569	−0.395
33	CH_2CH_2NHMe	$CH_2CH_2NHCH_2CH_2OH$	−0.118	−0.175	0.101	0.174
34	CH_2CH_2OH	$CH_2CH_2NMe_2$	1.721	1.416	1.311	1.803
35	CH_2CH_2OH	$CH_2CH_2NH_2$	1.947	2.249	2.356	1.828

[a] Experimental activity.
[b] 3D-HOV MLR predicted activity.
[c] 3D-HOV CV predicted activity.
[d] 3D-HOV PLS predicted activity.

2.2. QSAR calculation

Molecular steric structures of 35 Aza-APs bases were firstly auto-constructed by Chemoffice 10.0, and then optimized at AM1 level by MOPAC semi-experience quantum chemistry software in Chem3D. Then net electric charge of atoms was calculated in single-point form by Mulliken analysis. After the above two items were input, respectively, into the forms of Descartes coordinates and net electric charge amounts, 3D-HoVAIF descriptors were produced by applying 3D-HoVAI-F.EXE, an applied programme written by our laboratory. Removing all the empty items, there are ultimately 24 3D-HoVAIF descriptors corresponding to a molecule. Then multiple linear regression (MLR) statistical analysis, etc., was used to generate the QSAR model equations. In all equations, r^2 is the squared correction coefficient, S is the standard error of the estimates, F is the Fisher significance ratio and N is the number of cases used in the analysis.

2.3. Experimental data

The series of 35 2,5-disubstituted indazolo[4,3-g,h]isoquinolin-6(2H)-ones experimental data are obtained from papers published by Krapcho et al. [10] and studied by Slavov et al. [31], which well-expressed cytotoxicity against tumor cell line LoVo. IC_{50} is the drug concentration inhibiting 50% of cellular growth following 1 h of drug exposure, and log IC_{50} is used to calculate in this paper. The structure and cytotoxic activity data on LoVo tumor cell line for the studied series of 9-Aza-APs are given in Table 2. All thirty-five compounds from this data set were divided into training and test sets, the former set consisting of 24 randomly chosen compounds and the remaining in the latter set (Fig. 1 and Table 3).

3. Results and discussion

Original spatial structures of the 35 Aza-bioisosteres of anthrapyrazoles (Aza-APs) molecules are autogenerated by software Chemoffice 10.0, then implementing a molecular mechanic (MM) conformation optimization (adopting MM + force field), and then optimized at AM1 level by MOPAC half-experience quantum chemistry software in Chem3D. Simultaneously, atomic partial charges are calculated by Mulliken population analysis. Taking forms of Cartesian coordinates and partial charges, respectively, spatial position for each atom in a molecule and the atomic charges are input into C-edited program Focus_hovf, giving rise to 3D-HoVAIF descriptors of the molecular. Comprising 6 atom types as H, $C(sp^3)$, $C(sp^2)$, $O(sp^3)$, $O(sp^2)$ and F in the 35 Aza-APs, 141 empty items are found in the above-mentioned 165 3D-HoVAIF descriptors. Besides, two $O(sp^2)$ ($O(sp^2)$–$O(sp^2)$ and $O(sp^2)$–F) interaction items are regarded as zero due to their scarceness and a far remote distance in these 35 Aza-APs (van der Waals interaction is very sensitive to distance). Removing all the empty items, there are ultimately 24 3D-HoVAIF descriptors corresponding to a molecule. In early works, two partition manners were usually adopted on this sample set: one is the top 21 compounds as training set and the remains as test set and the other, the whole 35 molecules served as sample set to construct model. To comprehensively validate performance of 3D-HoVAIF, both these two partition manners are implemented here.

To facilitate comparison, different modeling methods as multiple linear regression (MLR) and partial least square (PLS) regression are employed, respectively. And MLR introduce variables in turn according to the values of Fisher prominent test by stepwise multiple regression (SMR), and in combination with leave-one-out cross-validation, the optimum variable number is determined in case the correlative coefficient firstly, the whole 35 molecules are utilized to construct model. Fig. 2 is the variables importance of projection through SMR. Figs. 3–5 plot the calculated against observed values for this sample set for the three linear 3D-HoVAIF models. Table 2 lists reference reports and our results for the 21 molecules in training set and the rests in predicting, showing 3D-HoVAIF model greatly gains by comparison, with its cross-validation $q^2 = 0.722$ better to the model reported by Slavov et al. [31], whose $q^2 = 0.38$ and $q^2 = 0.69$. The good cross-validation value shows our model has good modeling stabilities. And the correlation coefficient of SMR-MLR, SMR-CV, SMR-PLS model are 0.965, 0.775 and 0.865, respectively, and it is 0.96 in the study of Slavov et al. [31]. These results indicate that the 3D-HOV model is acceptable from statistical point of view.

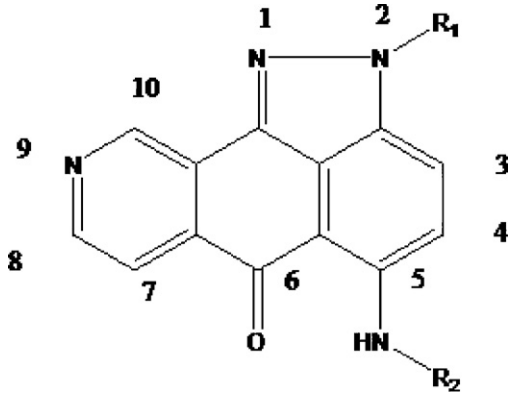

Fig. 1. General structural formula of 9-Aza-APs.

Table 3
Comparison between QSAR models of thirty-five 9-Aza-APs

No.	Model	n	R^2	q^2	S.D.	F
1	3D-HoVAIF[a]	35	0.965	\	0.289	21.734
2	3D-HoVAIF[b]	35	0.775	\	0.509	16.316
3	3D-HoVAIF[c]	35	0.865	0.722	0.299	\
4	Ref[d]	35	0.66	\	0.28	20.25
5	Ref[e]	35	0.67	0.38	\	\
6	Ref[f]	35	0.96	0.69	\	\

[a] SMR-MLR model.
[b] SMR-CV model.
[c] SMR-PLS model.
[d] 2D-Codessa.
[e] 3D-Steric Fields.
[f] 3D-Electrostatic Fields.

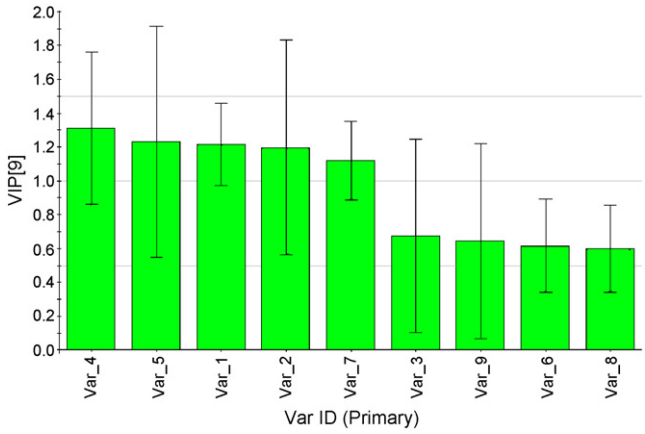

Fig. 2. Plot for variable importance of projection.

The best of SMR-PLS model equation (Eq. (4)) was selected for the further analysis. In this equation, $E_{3\text{-}7}$ means electrostatic interaction of the 3rd kind of atom and the 7th kind of atom (re. Table 1), $H_{5\text{-}5}$ represents hydrophobic interaction of the 5th kind of atom and the 5th kind of atom, and $S_{2\text{-}2}$ represents steric interaction of the 2nd kind of atom and the 2nd kind of atom, etc.

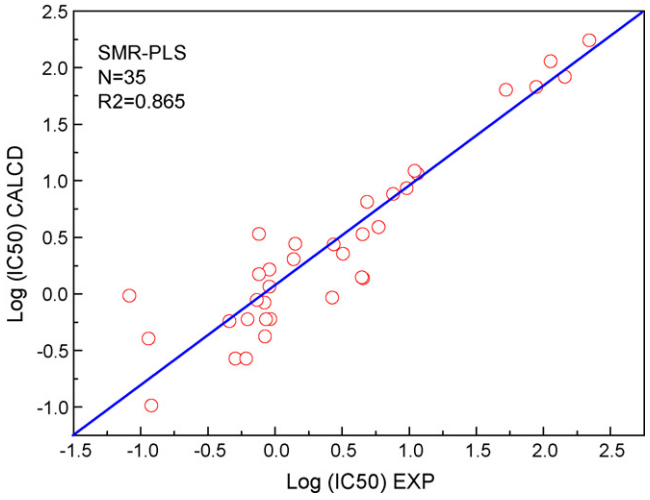

Fig. 3. Observed versus predicted values for the anticancer activity ($\log(IC_{50})$) of thirty-five 9-Aza-APs by SMR-PLS.

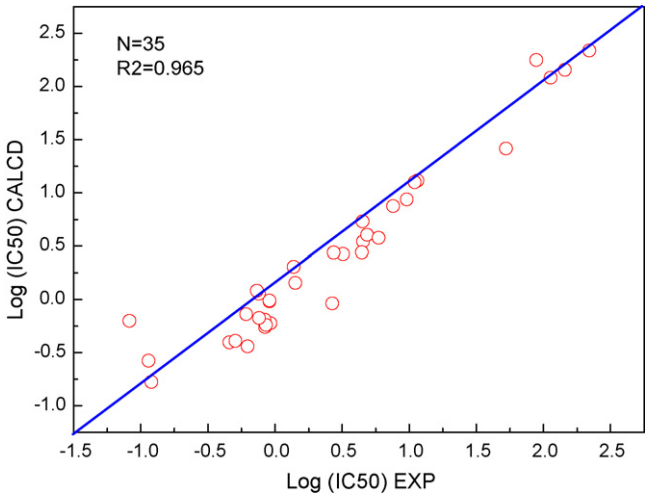

Fig. 4. Observed versus predicted values for the anticancer activity ($\log(IC_{50})$) of thirty-five 9-Aza-APs by SMR-MLR.

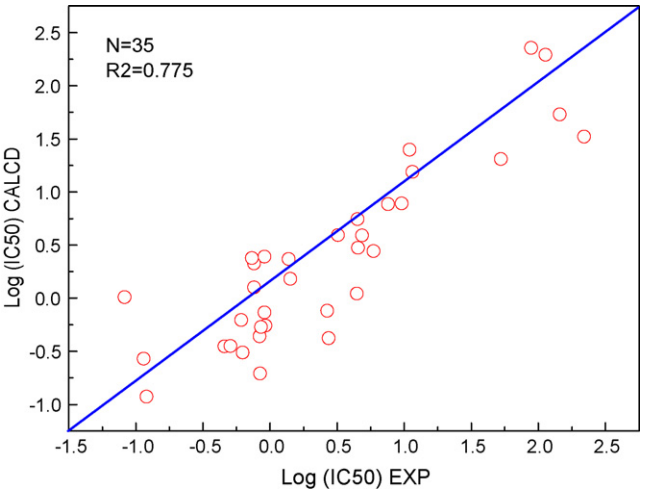

Fig. 5. Observed versus predicted values for the anticancer activity ($\log(IC_{50})$) of thirty-five 9-Aza-APs by SMR-CV.

$$\log(IC_{50}) = 0.482 + 5.703E_{3\text{-}7} - 0.0582H_{5\text{-}5} - 0.702E_{1\text{-}5} - 6.186E_{6\text{-}6} - 2.653H_{4\text{-}6} - 5.189S_{2\text{-}2} - 1.451E_{2\text{-}8} + 5.543E_{3\text{-}6} + 0.171S_{1\text{-}5} \quad (4)$$

According to the Eq. (4), we can find that there are nine variables appearing in this QSAR model. And the correspond-

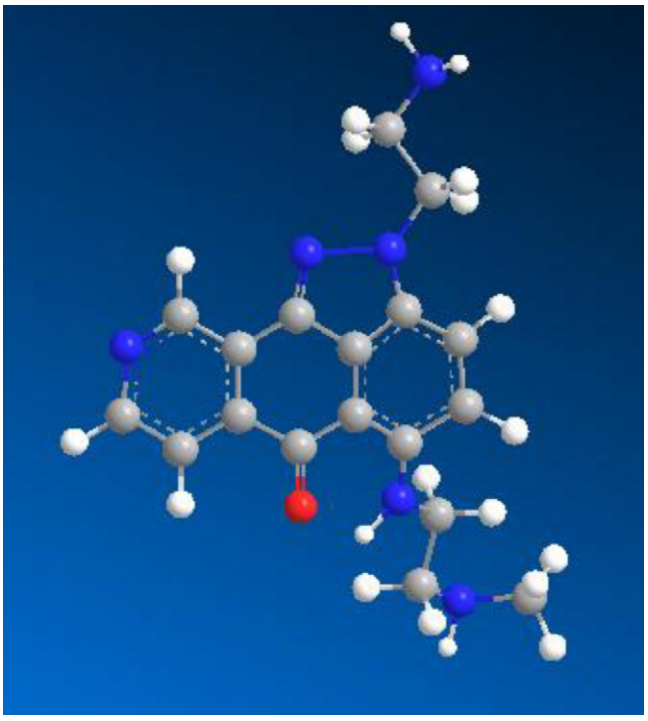

Fig. 6. The structure of the third molecular of 35 Aza-APs.

ing three-dimensional items are steric items of the $S_{2\text{-}2}$, $S_{1\text{-}5}$, electrostatic items of $E_{3\text{-}7}$, $E_{1\text{-}5}$, $E_{6\text{-}6}$, $E_{2\text{-}8}$, $E_{3\text{-}6}$, and hydrophobic items of the $H_{5\text{-}5}$, $H_{4\text{-}6}$, respectively. And the values for variable importance of projection are $E_{3\text{-}7}$ 1.3108, $H_{5\text{-}5}$ 1.22908, $E_{1\text{-}5}$ 1.21514, $E_{6\text{-}6}$ 1.19682, $H_{4\text{-}6}$ 1.11971, $S_{2\text{-}2}$ 0.675709, $E_{2\text{-}8}$ 0.644175, $E_{3\text{-}6}$ 0.614522, $S_{1\text{-}5}$ 0.599416, respectively, as we can find that electrostatic interaction has the most effect on molecular activity, and steric interaction and hydrophobic interaction have secondary impact. Furthermore, we can find out that the exist of amidocyanogen and the interaction between nitrogen atom and nitrogen atom have crucial effect on its anticancer ability, by analyzing atoms interaction in Table 1. And we find the whole matrix aromatic ring is also necessary to anticancer activity because of its hydrophobic effect, including the electrostatic interaction of the C = N bond. All these structures are found in the 3rd molecular (Fig. 6), which has the highest anticancer in this series compounds.

4. Conclusion

The 3D-HoVAIF methods presented are developed here for Aza-bioisosteres of anthrapyrazoles (Aza-APs) as anticancer agents, and satisfying model results have been obtained. Synchronously, the three-dimensional quantitative structure–activity relationship is a useful tool in the design of novel compounds with regard to the placement of functional groups, showing which areas of the compound could be responsible for the differing activities of the training set of molecules. It's believed 3D-HOV QSAR approach can be introduced into more molecular system improvement and it has three main points as follow:

(a) Atoms are typed for 10 kinds according to their families in periodic table of elements and self-hybridization states.
(b) Three non-bonded (electrostatic, van der Waals and hydrophobic) factors, directly related to bioactivities, are utilized to express intramolecular potential energies.
(c) Based on molecular steric structures, 165 non-bond interaction items calculated are taken as the three-dimensional (3D) structural descriptors of the molecule.

Acknowledgements

The authors thank the Foundations of National High Technology (863) Programme (Grant No. 2006AA02Z312), State Key Laboratory of Chemo/Biosensing and Chemometrics Fund (Grant No.2005012) and Chongqing University Juche Innovation Fund (Grant No. 200707282).

References

[1] H. Malonne, G. Atassi, DNA topoisomerase targeting drugs: mechanisms of action and perspectives, J. Anti-Cancer Drugs 8 (9) (1997) 811–822.
[2] A.P. Krapcho, M.J. Maresch, M.P. Hacker, L. Hazelhurst, E. Menta, A. Oliva, S. Spinelli, G. Beggiolin, F.C. Giuliani, G. Pezzoni, S. Tognella, Anthracene-9,10-diones and aza bioisosteres as antitumor agents, Curr. Med. Chem. 2 (1995) 803–824.
[3] F. Arcamone, S. Penco, Synthesys of new doxorubicin analogs, in: J.W. Lown (Ed.), Anthracycline and Anthracendione-based Anticancer Agents, Elsevier, New York, 1988.
[4] R.K.Y. Zee-Cheng, C.C. Cheng, Anthraquinone anticancer agents, Drugs Fut. 8 (1983) 229–248.
[5] S.K. Sengupta, Topoisomerase II Inhibitors, in: W.O. Foye (Ed.), Cancer Chemotherapeutic Agents, Am. Chem. Soc., Washington, DC, 1995, pp. 205–260.
[6] D. Faulds, J.A. Balfour, P. Chrisp, H.D. Langtry, Mitoxantrone: a review of its pharmacodynamic and pharmacokinetic properties, and therapeutic potential in the chemotherapy of cancer, Drugs 41 (1991) 400–449.
[7] M. Palumbo, B. Gatto, C. Sissi, DNA topoisomerase-targeted drugs, in: M. Demeunynch, C. Bailly, W.D. Wilson (Eds.), DNA and RNA Binders, vol. 1, From Small Molecules to Drugs, Wiley-VCH, 2002, pp. 503–507.
[8] W.H. Frishman, H.M. Sung, H.C. Yee, L.L. Liu, D. Keefe, A.I. Einzig, J. Dutcher, Cardiovascular toxicity with cancer chemotherapy, Curr. Probl. Cancer. 21 (1997) 301–330.
[9] A.P. Krapcho, E. Menta, Antitumor aza-anthrapyrazoles, Drugs Fut. 22 (1997) 641–646.
[10] A.P. Krapcho, E. Menta, A. Oliva, D.R. Domenico, L. Fiocchi, E. Maresch, C.E. Gallagher, M.P. Hacker, G. Beggiolin, F.C. Giuliani, G. Pezzoni, S. Spinelli, Synthesis and Antitumor Evaluation of 2,5-Disubstituted-Indazolo[4,3-*gh*]isoquinolin-6(2*H*)-ones (9-Aza-anthrapyrazoles), J. Med. Chem. 41 (1998) 5429–5444.
[11] C. Sissi, S. Moro, S. Richter, B. Gatto, E. Menta, S. Spinelli, A.P. Krapcho, F. Zunino, M. Palumbo, Biophysical and biochemical studies relevant to the mechanism of action, Mol. Pharmacol. 59 (2001) 96–103.
[12] A. Liwo, D. Jeziorek, T. Ossowski, D. Dyl, A. Tempczik, J. Tarasuik, M. Nowacka, E. Borowski, W. Woznicki, Acta Biochem. Pol. 42 (1995) 445–456.
[13] R. Supino, D. Polizzi, R. Pavesi, G. Pratesi, F. Guano, G. Capranico, M. Palumbo, C. Sissi, S. Richter, G. Beggiolin, E. Menta, G. Pezzoni, S. Spinelli, D. Torriani, N. Carenini, B.L. Dal, F. Facchinetti, M. Tortoreto, F. Zunino, Book reviews, Oncology 61 (2001) 234–242.
[14] C. Hansch, A. Leo, Substituent Constants for Correlation Analysis in Chemistry and Biology, John Wiley & Sons, New York, 1979, pp. 1–329.
[15] H. Winer, Cis-and trans-piperylenes, J. Am. Chem. Soc. 69 (1947) 2636–2641.
[16] H. Hosoya, A newly proposed quantity characterizing the topological nature of structural isomers of saturated hydrocarbons, Bull. Chem. Soc. 44 (1971) 2332–2339.
[17] M. Randic, On characterization of molecular branching, J. Am. Chem. Soc. 97 (1975) 6609–6615.
[18] A.T. Balaban, Highly discriminating distance-based topological index, Chem. Phys. Lett. 89 (1982) 399–404.
[19] A.R. Katritzky, U. Maran, S. Victor, M. Karelson, Structurally diverse QSPR correlations of technologically relevant physical properties, J. Chem. Inf. Comput. Sci. 40 (2000) 1–18.
[20] R.D. Cramer, D.E. Patterso, J.D. Bunce, Comparative molecular field analysis (CoMFA). 1. Effect of shape on binding of steroids to carrier proteins, J. Am. Chem. Soc. 110 (1988) 5959–5967.
[21] G. Klebe, U. Abraham, T. Mietzner, Molecular similarity indices in a comparative analysis (CoMSIA) of drug molecules to correlate and predict their biological activity, J. Med. Chem. 37 (1994) 4130–4146.
[22] A.M. Doweyko, The hypothetical active site lattice-an approach to modelling active sites from data on inhibitor molecules, J. Med. Chem. 31 (1988) 1396–1406.
[23] P.J. Goodford, A computational procedure for determining energetically favorable binding sites on biologically important molecules, J. Med. Chem. 28 (1985) 849–857.
[24] W. Hasel, T.F. Hendrikson, W.C. Still, A rapid approximation to the solvent accessible surface areas of atoms, Tetrahedron. Comput. Methodol. 1 (1988) 103–116.
[25] J. Pei, Q. Wang, J. Zhou, L. Lai, protein-ligand binding free energy: atomic solvation parameters for partition coefficient and solvation free energy calculation, Proteins 57 (2004) 651–664.

[26] G.E. Kellogg, S.F. Semus, D.J. Abraham, HINT-a new method of empiric alhydrophobic field calculation for CoMFA, J. Comput-Aided Mol. Des. 5 (1991) 545–552.
[27] F.C. Wireko, G.E. Kellogg, D.J. Abraham, Allosteric modifiers of hemoglobin. 2. Crystallographically determined binding sites and hydrophobic binding/interaction analysis of novel hemoglobin oxygen effectors, J. Med. Chem. 34 (1991) 758–767.
[28] G.E. Kellogg, G.S. Joshi, D.J. Abraham, New tools for modeling and understanding hydrophobicity and hydrophobic interactions, Med. Chem. Res. 1 (1992) 444–453.
[29] G.E. Kellogg, D.J. Abraham, K. Lock, S. Lock, Complementary hydrophobicity map predictions of drug structure from a known receptor/receptor structure from known drugs, J. Mol. Graph. 10 (1992) 212–217.
[30] V.R. Nayak, G.E. Kellogg, Cyclodextrin-barbiturate inclusion complexes: a CoMFA/HINT 3D QSAR study, Med. Chem. Res. 3 (1994) 491–502.
[31] S. Slavov, M. Atanasova, B. Galabov, QSAR analysis of the anticancer activity of 2,5-disubstituted 9-Aza-anthrapyrazoles, QSAR Comb. Sci. 2 (2007) 173–181.